Bull Volcanol (2015) 77: 51
DOI 10.1007/s00445-015-0937-8

RESEARCH ARTICLE

The historical (218±14 aBP) explosive eruption of Tutupaca volcano (Southern Peru)

Pablo Samaniego[1] · Patricio Valderrama[1,2] · Jersy Mariño[2] · Benjamín van Wyk de Vries[1] · Olivier Roche[1] · Nélida Manrique[2] · Corentin Chédeville[1] · Céline Liorzou[3] · Lionel Fidel[2] · Judicaëlle Malnati[1]

Received: 22 January 2015 / Accepted: 14 May 2015 / Published online: 24 May 2015

Abstract The little known Tutupaca volcano (17° 01′ S, 70° 21′ W), located at the southern end of the Peruvian arc, is a dacitic dome complex that experienced a large explosive eruption during historical times. Based on historic chronicles and our radiometric data, this eruption occurred 218±14 aBP, probably between 1787 and 1802 AD. This eruption was characterised by a large sector collapse that triggered a small debris avalanche (<1 km^3) and an associated pyroclastic eruption whose bulk volume was 6.5–7.5×10^7 m^3. Both units were emplaced synchronously and spread onto the plain situated to the northeast of Tutupaca volcano. The spatial and temporal relationship between the debris avalanche and the pyroclastic density current deposits, coupled with the petrological similarity between the juvenile fragments in the debris avalanche, the pyroclastic density current deposits and the pre-avalanche domes, indicates that juvenile magma was involved in the sector collapse. Large amounts of hydrothermally altered material are also found in the avalanche deposit. Thus, the ascent of a dacitic magma, coupled with the fact that the Tutupaca dome complex was constructed on top of an older, altered volcanic sequence, probably induced the destabilisation of the hydrothermally active edifice, producing the debris avalanche and its related pyroclastic density currents. This eruption probably represents the youngest debris avalanche in the Andes and was accompanied by one of the larger explosive events to have occurred in Southern Peru during historical times.

Keywords Tutupaca · Peru · Central Andes · Explosive activity · Sector collapse · Volcanic hazards · Historical activity

Editorial responsibility: S. De la Cruz-Reyna

✉ Pablo Samaniego
pablo.samaniego@ird.fr

[1] Laboratoire Magmas et Volcans, Université Blaise Pascal-CNRS-IRD, 5 rue Kessler, 63038 Clermont-Ferrand, France

[2] Observatorio Vulcanológico del INGEMMET, Dirección de Geología Ambiental y Riesgo Geológico, Urb. Magisterial B-16, Umacollo, Arequipa, Peru

[3] Université de Brest, CNRS, UMR 6538 Domaines Océaniques, Institut Universitaire Européen de la Mer, Place Copernic, F-29280 Plouzané, France

Introduction

The Peruvian volcanic arc results from the subduction of the oceanic Nazca plate beneath South-American continental lithosphere. This volcanic province, which belongs to the Central Volcanic Zone of the Andes, is formed upon the Western Cordillera of the Peruvian Andes, and it comprises at least 12 Late Pleistocene and Holocene volcanic centres and several monogenetic fields (Siebert et al. 2010). Among these volcanic centres, seven volcanoes have experienced eruptive activity since the arrival of the Spanish conquistadors in the sixteenth century. These edifices include the well-know El Misti, Ubinas, Sabancaya and Huaynaputina volcanoes, as well as other lesser-studied edifices such as Ticsani, Tutupaca and Yucamane (Fig. 1).

On the basis of numerous studies over the last decades, the eruptive chronologies of a number of these volcanic centres are well constrained. The two last major explosive events in this part of the Andes were the large 2-ka BP plinian eruption of El Misti volcano (Volcanic Explosive Index-VEI of 5; Thouret et al. 2001; Harpel et al. 2011; Cobeñas et al. 2012) and the 1600 AD explosive eruption of Huaynaputina volcano which was the biggest historical explosive eruption in the

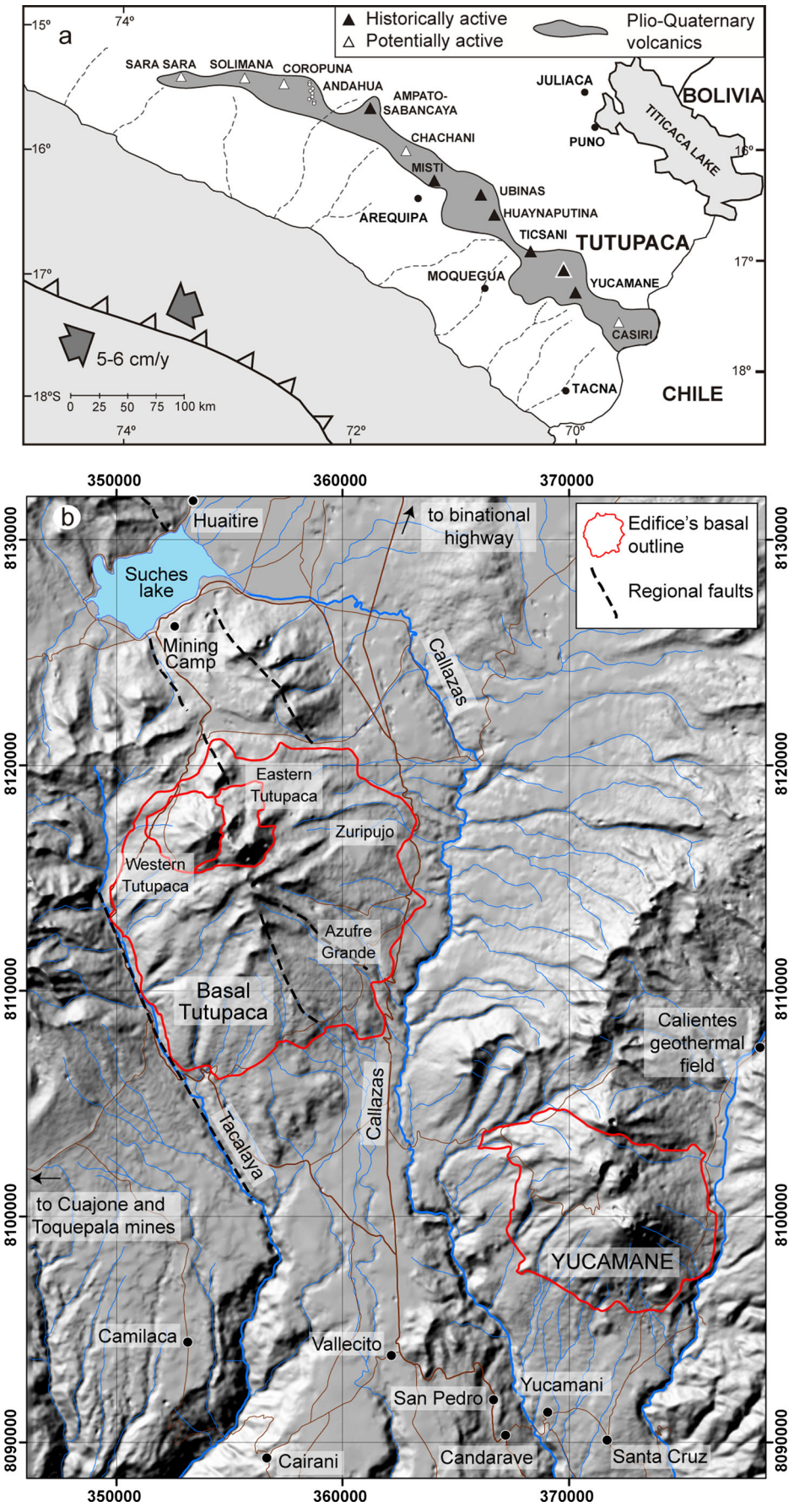
a
Historically active
Potentially active
Plio-Quaternary volcanics
SARA SARA
SOLIMANA
COROPUNA
ANDAHUA
AMPATO-SABANCAYA
CHACHANI
MISTI
UBINAS
HUAYNAPUTINA
TICSANI
AREQUIPA
MOQUEGUA
TUTUPACA
YUCAMANE
CASIRI
TACNA
JULIACA
PUNO
TITICACA LAKE
BOLIVIA
CHILE
5-6 cm/y
0 25 50 75 100 km
b
Huaitire
to binational highway
Edifice's basal outline
Regional faults
Suches lake
Mining Camp
Callazas
Eastern Tutupaca
Zuripujo
Western Tutupaca
Azufre Grande
Basal Tutupaca
Calientes geothermal field
Tacalaya
to Cuajone and Toquepala mines
YUCAMANE
Camilaca
Vallecito
San Pedro
Yucamani
Cairani
Candarave
Santa Cruz
350000
360000
370000
8130000
8120000
8110000
8100000
8090000

◀ **Fig. 1** **a** Location of Tutupaca volcano in the Peruvian volcanic arc. **b** Regional map showing the location of the Tutupaca and Yucamane volcanoes

Andes (VEI 6, Thouret et al. 1999; Adams et al. 2001). Other small to moderate explosive events occurred at El Misti in the 15th century (Thouret et al. 2001), as well as at the frequently active Ubinas edifice that experienced at least 25 eruptive episodes since the 16th century (Thouret et al. 2005; Siebert et al. 2010) including a moderate-size eruption in 1667 AD and the recent eruptions of AD 2006–2009 and 2013–2015 (Rivera et al. 2014). Last, rare historical accounts suggest that Sabancaya volcano was also active in the 18th century (AD 1750, 1784), and more recently, vulcanian explosive activity was described in AD 1988–1997 (Siebert et al. 2010; Gerbe and Thouret 2004). All this information shows that the Peruvian segment of the Andean Central Volcanic Zone experienced significant explosive activity through the last few centuries.

Tutupaca volcano (17° 01′ S, 70° 21′ W) is located at the southern end of the Peruvian arc (Fig. 1), 25–30 km to the north of Candarave village (Tacna Department, Southern Peru). Historical chronicles reported by Hantke and Parodi (1966) indicate that several volcanic eruptions affected this part of the Andes in AD 1780, 1787, 1802, 1862, and 1902. These authors suggested that the source of these eruptions was Tutupaca volcano. However, based on the youthful and uneroded morphology of the contiguous Yucamane volcano, several authors attributed these eruptions to the latter (Siebert et al. 2010; de Silva and Francis 1990). In this manuscript, we present results of a detailed study of recent Tutupaca eruptive products, which include field descriptions of the main volcanic units, petrologic characterisation of juvenile material, radiocarbon dating and correlation with historical records. With these results, we reconstruct the eruptive sequence associated with the last eruption of Tutupaca, which is an unidentified historical explosive event in the Andes.

Overall structure of Tutupaca volcano

The Tutupaca volcanic complex is constructed on top of a high volcanic plateau consisting of volcanic and volcano-sedimentary rocks, which include thick Mio-Pliocene ignimbritic deposits (Fidel and Zavala 2001; Mamani et al. 2010). This sequence is well exposed in the Callazas and Tacalaya valleys located at the eastern and western parts of the complex (Fig. 1). The Tutupaca volcanic complex rises from the basement at 4400–4600 m above sea level (m asl) and is composed of a big basal edifice and two small "twin" peaks (the Western and Eastern Tutupaca), which are located at the northern part of the volcanic complex and constructed on the remnants of the basal volcano (Figs. 1 and 2). Several fault systems have been identified in this part of the Andean cordillera, the main one being a series of normal faults with a sinistral component that has been mapped around the Suches lake and that displays a roughly N140 direction (Benavente et al. 2010). These faults affected the volcanic complex and seem to have influenced its structural development (Fig. 1).

The *Basal Tutupaca* edifice is mostly composed of andesitic and dacitic lava flows. Based on the radial distribution and dips of these lavas, we infer that the former summit was located 2–3 km to the south of the current Tutupaca peaks. The summit zone is characterised by an uneven topography and strong hydrothermal alteration (Figs. 1 and 2). This edifice was strongly affected by Pleistocene glaciation, resulting in the highly eroded morphology and glacial modification of several radially oriented valleys. As a result, major moraine deposits (up to 100 m thick) were stacked mostly in the southern part of the complex, as well as in the Callazas and Tacalaya valleys. These moraines are probably formed during the Last Glacial Maximum (LGM), which has been broadly dated at 17–25 ka in the Western Cordillera of the Peruvian Andes (Smith et al. 2008; Bromley et al. 2009). In addition, a thick ignimbrite deposit of dacitic composition outcrops on the southern and western flanks of the edifice and represents a major explosive phase that probably occurred at the end of edifice evolution. This ignimbrite deposit is covered by the

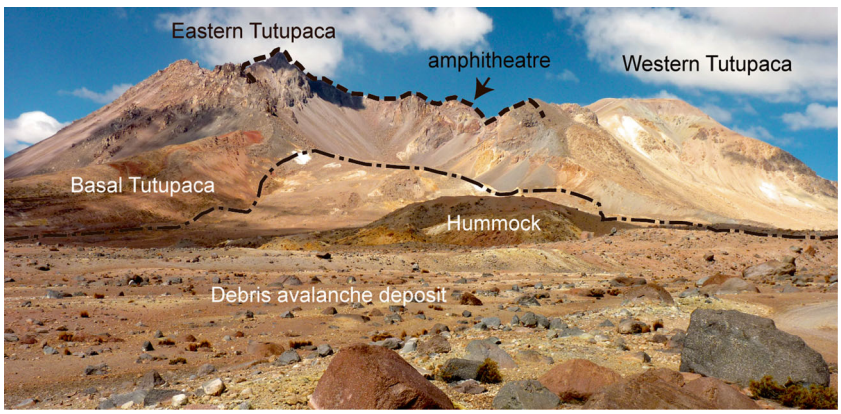

Fig. 2 Panoramic view of the north-east of Tutupaca volcano and its amphitheatre

LGM moraines, suggesting an age older than 25 ka. The less massive *Western Tutupaca* peak (5815 m asl) is mostly composed of lava flows and domes of siliceous andesitic and dacitic compositions. This edifice was also eroded by the Late Pleistocene glaciers. A sequence of tephra fallout deposits outcropping in the distal south-western part of the volcano shows that this edifice experienced powerful plinian to subplinian eruptions during its history. Last, the younger *Eastern Tutupaca* peak (5790 m asl) is a dacitic dome complex characterised by a lack of glacial erosion, suggesting a Holocene age. It is composed of at least 7 coalescing lava domes (Manrique 2013), which are cut by a 1-km-wide horseshoe-shaped amphitheatre open to the NE (Fig. 1b). It is worth noting that the direction of opening of the amphitheatre is almost orthogonal to the N140 regional faults that cut the edifice. We identified at least two debris avalanche deposits associated with this edifice: an older deposit that is channelised in the valleys located to the E (Zuripujo) and SE of the volcano (e.g. Azufre Grande) and a younger deposit that outcrops immediately to the NE of the amphitheatre and that will be described in detail in this work.

The recent eruptive products

The north-eastern part of Eastern Tutupaca edifice (Figs. 2 and 3) exhibits a remarkably well-preserved volcanic sequence characterised by abundant surface structures. Here, we describe the main characteristics of these deposits in stratigraphic order. The detailed descriptions of these deposits and their surface structures, as well as their dynamic implications, are beyond the scope of this manuscript and are discussed in a companion paper (Valderrama et al. 2014).

The Zuripujo pyroclastic density current deposit (Z-PDC)

Exposed in the lower part of the Zuripujo valley, 8–10 km from the Eastern Tutupaca edifice, is a 2–5-m-thick unit composed of at least two or three block-and-ash flow deposits, which are interlayered with centimetre-thick ash-rich layers showing cross-bedding and lamination (Figs. 3, 4 and 5). The block-and-ash flow deposits are massive, matrix-supported, with 20–30 vol.% angular and subangular blocks in an unconsolidated, grey, medium ash matrix. The block sizes range from 5 to 10 cm, although 1-m diameter blocks are also locally observed. The deposit is mostly polylithologic, but the most common lithology is dark grey, unaltered, dense dacitic blocks with plagioclase, amphibole and biotite in a vitreous groundmass. These blocks, and the breadcrust bombs also locally observed, are interpreted as representing a collapsing dome. A large amount of slightly altered, dark grey, pyroxene-rich andesitic blocks are also present in the deposit and are interpreted as blocks entrained from underlying units of the older edifice. The most striking characteristic of this deposit, however, is the relatively large amount (5–10 vol.%) of centimetre-size, white-yellowish, highly altered, friable lava fragments that are also present as smaller clasts in the matrix of the deposit (Fig. 5). Three charcoal samples collected in this unit have been dated and yielded almost identical ages (190± 30, 220±30 and 230±30 aBP; Table 1). At the Zuripujo valley, the Z-PDC unit is overlain by an up to 1-m-thick (Figs. 4 and 5), locally reworked, grey-reddish ash-rich layer that includes some breadcrust bombs at the top and is interpreted as a lateral facies of the Paipatja pyroclastic density current deposit (P-PDC, see below). The contact between these two units is commonly flat, although in rare outcrops, we observed erosive features as well as a 10–30-cm-thick layer of reworked material.

The upper part of the Zuripujo valley exposes a 3–5-m-thick sequence of block-and-ash flow deposits that covers an older debris avalanche deposit. This block-and-ash unit, which can be traced up to the eastern foot of the Tutupaca domes, displays a rough surface morphology characterised by an enrichment in metric-size angular blocks and flow structures such as the fan observed at the Zuripujo valley bifurcation, 4–5 km from the Eastern Tutupaca summit. The spatial continuity between the proximal and distal deposits at Zuripujo valley, its stratigraphic position (both covered by the Paipatja PFD) and the petrography of the blocks indicate that they are parts of the same volcanic unit.

The Tutupaca debris avalanche deposits

This unit is exposed towards the northeast of the Tutupaca dome complex, in a zone between the amphitheatre and the Villaque and Taipicirca hills (Fig. 3), over an area of around 12–13 km^2. In the proximal zone (i.e. the first 3 km from the Tutupaca amphitheatre), a heterogeneous breccia is exposed, composed of two successive units interpreted as debris avalanche deposits. At the foot of the amphitheatre, the lower unit forms a massive, Toreva block-like structure 1–1.5 km in diameter and 150–200 m high that is flanked by two 1.5-km-long levees diverging from the amphitheatre. Downhill, the deposit consists of several 200–700-m-long, 20–40-m-high megablocks, as well as smaller 100–200-m-long hummock-like hills (Figs. 3, 4 and 6). These features are composed of a heterogeneous, polymict breccia, which, following Glicken's (1991) facies terminology, is a block facies consisting of highly cataclased, metric-size blocks with abundant jigsaw cracks in a fine-medium sand matrix. Lava blocks are mostly highly altered (hydrothermally altered), yellow-reddish andesites, although other petrographic types are observed and include oxidised, reddish-grey andesites, and scarce, unaltered, dark grey andesites and dacites. Given the high amount of altered fragments, we call this unit the Hydrothermally-Altered Debris Avalanche Deposit (HA-DAD, Fig. 6).

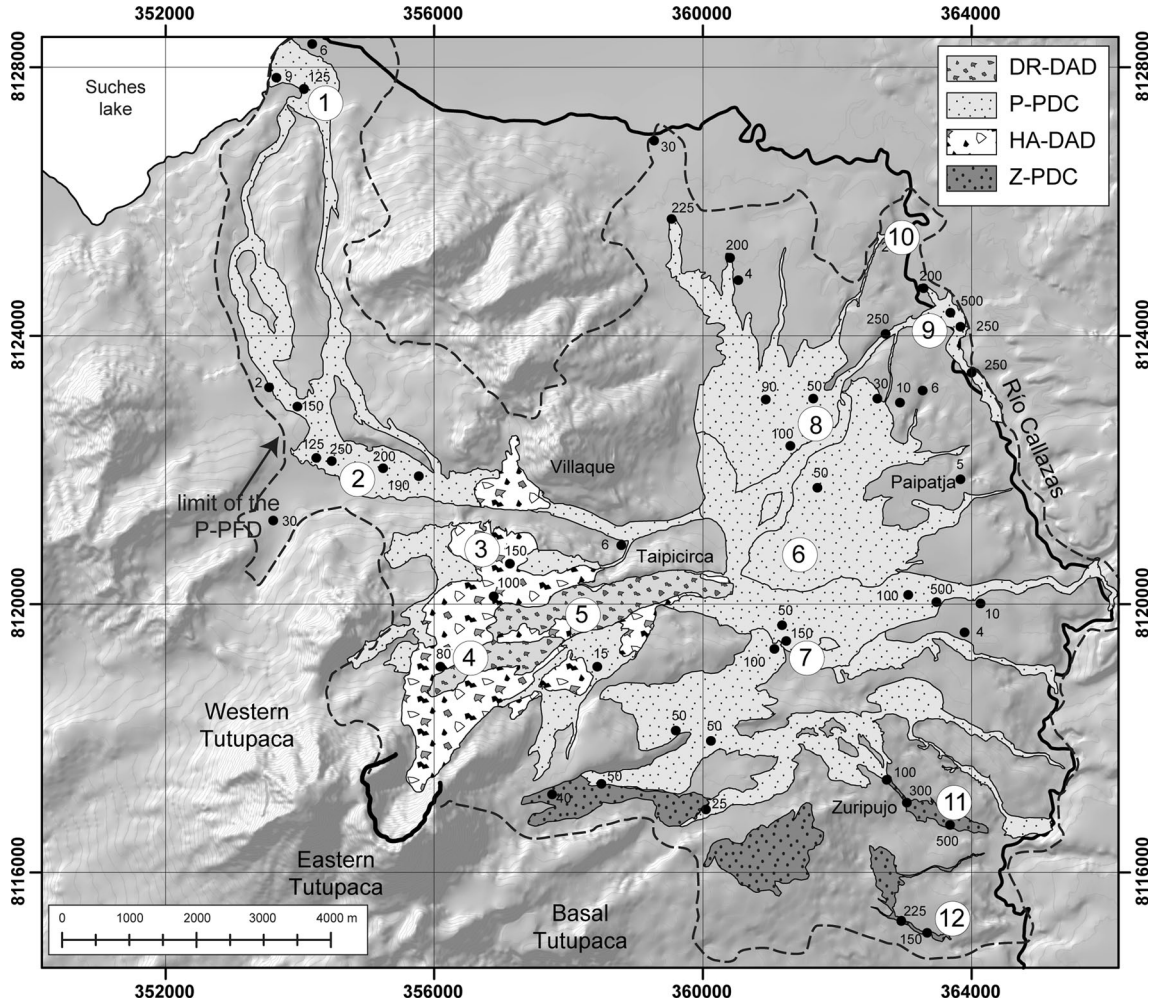

Fig. 3 Simplified geological map of the Recent Tutupaca deposits. Location of main stratigrafic sections is shown. *Z-PDC* Zuripujo pyroclastic density current deposit, *HA-DAD* hydrothermally altered debris avalanche deposit, *P-PDC* Paipatja pyroclastic density current deposit, *DR-DAD* dome-rich debris avalanche deposit. The area delimited by the *black dashed line* corresponds to the lateral and distal deposits related to the ash-cloud accompanying the P-PDC. *Dots* correspond to minimum thickness (in cm) of P-PDC

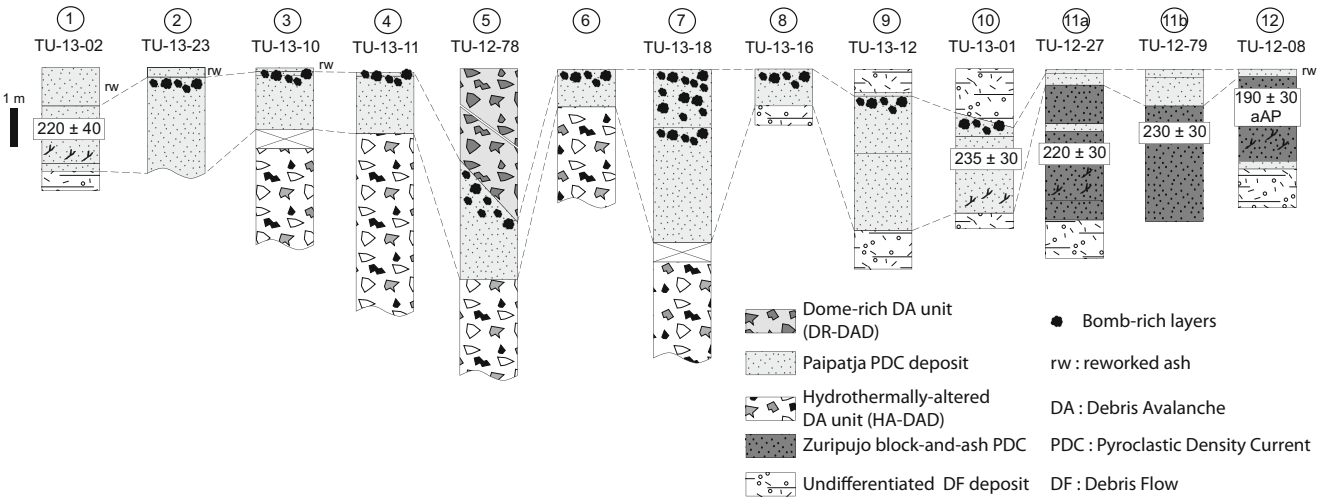

Fig. 4 Composite stratigraphic sections of the Tutupaca debris avalanche deposits and related pyroclastic flow deposits. Location of the stratigraphic sections is shown in Fig. 3

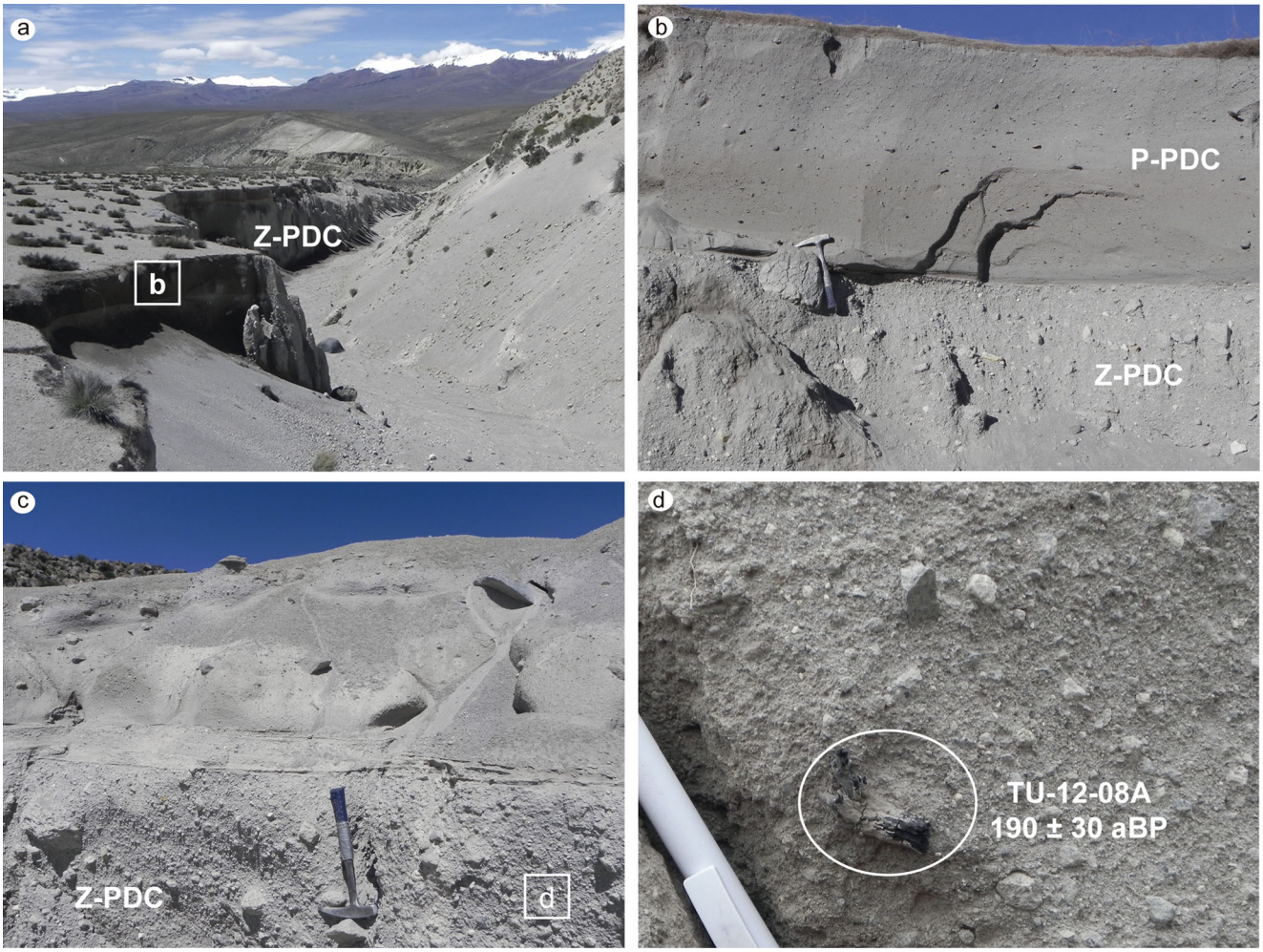

Fig. 5 Photos of the Zuripujo pyroclastic density current deposit (Z-PDC). **a** Outcrop of 4–5-m-thick outcrop of Z-PDC in the Zuripujo valley (site 11, samples TU-12-27 and TU-12-79, Fig. 3). **b** The upper 2 m of outcrop (**a**) showing the Z-PDC overlain by the Paipatja pyroclastic density current deposit (P-PDC). Note the presence of breadcrust bombs in the Z-PDC. **c** The Z-PDC at a small ravine located to the south of the main Zuripujo valley (site 12, sample TU-12-08, Fig. 3). **d** Detail of the matrix of the Z-PDC deposit showing a charcoal fragment. Note also the abundance of light-coloured hydrothermally altered fragments

In the medial zone (i.e. roughly 3 to 6 km from the amphitheatre), the debris avalanche deposit is characterised by a rough surface morphology consisting of longitudinal, elongated ridges that commonly diverge with distance from the amphitheatre (Figs. 3 and 6). These ridges are 5–10 m wide, 150–400 m long and 2–5 m high (for a detailed description of these structures, the reader is referred to the companion paper of Valderrama et al. (2014)). In this medial zone, the debris avalanche deposit is exposed along two corridors. The first one follows an NNE direction, reaching the Taipicirca valley and defining an 80-m-high run-up onto the Villaque hill, whereas the second corridor is between two old moraines and follows an NE direction to reach the Paipatja plain. In this latter part, the HA-DAD unit is overlain by an upper deposit, which is mainly composed of unaltered (fresh) dark grey dome rocks of dacitic composition (Dome-Rich Debris Avalanche Deposit, DR-DAD, Fig. 6). This upper unit shows scarce evidence of cataclasis (such as jigsaw cracks), but instead shows abundant prismatically jointed blocks, indicating an origin in a still-hot dome complex. In between these two DAD units, we observed the Paipatja pyroclastic flow deposit described below.

Last, in the distal zone (i.e. more than 6 km from the amphitheatre), on the Paipatja plain and up to the Callazas river, the debris avalanche deposits are mostly covered by the Paipatja pyroclastic flow deposits (see below). Several big (>1 m in diameter) blocks distributed on the plain, whose bases are surrounded by the Paipatja pyroclastic flow deposit, suggest, however, that there is an underlying debris avalanche deposit up to a distance of 7–8 km from the amphitheatre. We estimate a volume of 0.6–0.8 km^3 on the basis of the mapped surface of the debris avalanche deposits and an average thickness of 25–40 m. This estimate probably represents a minimum volume, given that the Tutupaca debris avalanche deposit is covered by the Paipatja pyroclastic flow deposits.

Table 1 ^{14}C age results obtained in this study

Sample No.	Lab code	Locality	UTM Easting	UTM Northing	Unit	Type of sample	^{14}C age (a BP)	$\partial^{13}C$ (o/oo)	Calendar age range (cal AD) - 1 sigma -	Relative area (%)	Calendar age range (cal AD) - 2 sigma -	Relative area (%)
TU-12-08A	GrA 55325	Candarave-Huaytire road	363234	8114941	Zuripujo PDC	charcoal	190±30	−22.12	1670-1700	25	1664-1816	68
									1722-1782	42	1828-1893	20
									1795-1809	12		
									1838-1845	4		
									1867-1878	6		
TU-12-27B	GrA 54421	Qda. Zuripujo	363116	8116729	Zuripujo PDC	charcoal	220±30	-	1665-1679	15	1645-1700	27
									1733-1800	85	1721-1810	67
TU-12-79B	GrA 56328	Qda. Zuripujo	363178	8116684	Zuripujo PDC	charcoal	230±30	−21.80	1662-1675	17	1641-1698	30
									1738-1798	83	1723-1808	69
TU-13-01A	GrA 60691	Paipatja plain	362912	8125348	Paipatja PDC	charcoal	235±35	-	1654-1675	26	1636-1700	32
									1739-1798	74	1721-1810	64
TU-13-02B	GrA 57883	Suches lake	354047	8127482	Paipatja PDC	charcoal	220±40	-	1652-1688	28	1642-1712	28
									1728-1804	72	1717-1814	56
											1834-1891	10
Average							218±14		1671-1675	7	1662-1680	15
									1739-1783	85	1731-1802	85
									1795-1798	8		

These AMS ages were calculated at the Center for Isotope Research of the University of Groningen, Netherlands by the team of the Prof. J. van der Plicht. UTM coordinates correspond to the WGS 1984 projection (zone 19)

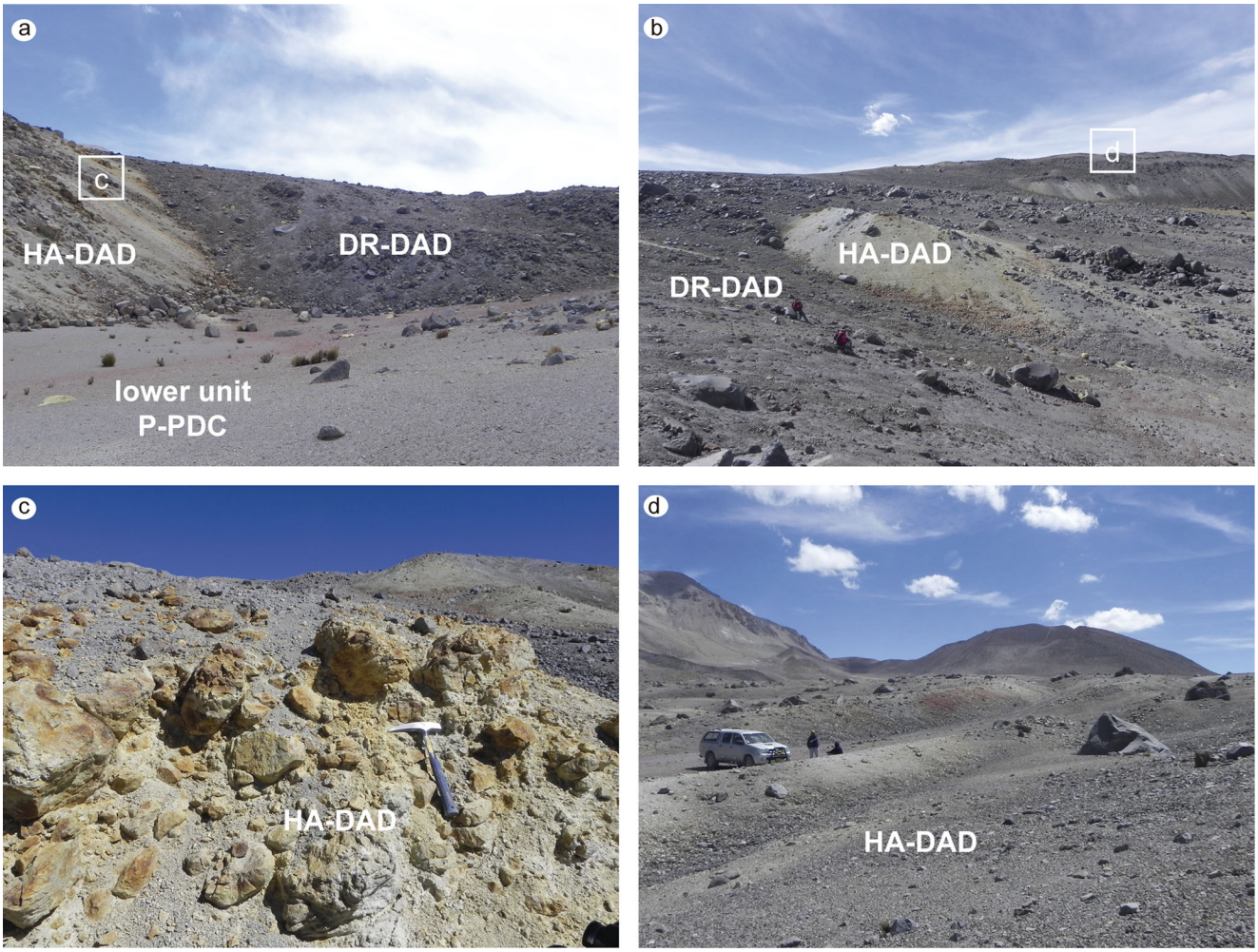

Fig. 6 Photos of the debris avalanche deposit (DAD) corresponding to the proximal-medial zone (site 5, Fig. 3). **a**, **b** Lower hydrothermally altered unit (HA-DAD) and upper dome-rich unit (DR-DAD). We also note the deposits of the P-PDC. **c** Detail of the HA-DAD showing the large amount of altered blocks. **d** Surface structures (ridges) observed at HA-DAD

The Paipatja pyroclastic density current deposit (P-PDC)

Distribution and stratigraphic relations

This unit spreads to the northeast of Tutupaca, reaching the Paipatja plain and the Callazas valley 8–10 km from the vent. A secondary branch of this unit reaches Suches lake 10–12 km from the vent (Fig. 3). In the proximal and medial zones (up to 6 km from the amphitheatre), this unit overlies the lower debris avalanche deposit unit (HA-DAD) and is covered by (and in some places interstratified with) the upper debris avalanche deposit unit (DR-DAD). In the distal zone (i.e. beyond 6 km from the amphitheatre), the P-PDC deposit also covers the main HA-DAD unit and appears to be mainly channelised in the numerous valleys draining the Paipatja plain, although an ash-rich, 10–20-cm-thick, over-bank deposit is also observed (Fig. 3). On the Paipatja plain, we observed two successive P-PDC units (Figs. 4 and 7). The widespread, lower unit covers the entire Paipatja plain and reaches the Callazas valley, whereas the upper unit is characterised by 1–1.5-m-thick bomb-rich lobes that overlie the lower unit (Figs. 4 and 7).

The thickness of the P-PDC unit is highly variable, ranging from 0.5 to 2 m thick on the Paipatja plain and around Suches Lake, to 2–5 m in the channelised distal zone in the Callazas valley. In addition, given that the P-PDC unit overrides the lower debris avalanche unit in the medial zone, it is less thick on the ridges than between them. As a result, large thickness variations (from around 10 cm to 1 m) are also observed on a scale as small as ~10 m. We stress that due to a lack of erosion, no cross sections exist in the flat area of the Paipatja plain and thus thickness measurements are scarce.

Deposit description and dating

Over the whole Paipatja plain, the P-PDC deposit is massive, matrix-supported, with 20–40 vol.% of angular to subangular lava blocks and bombs in a dark grey, medium-to-coarse ash matrix. Block size ranges from ~3 to 20 cm, although

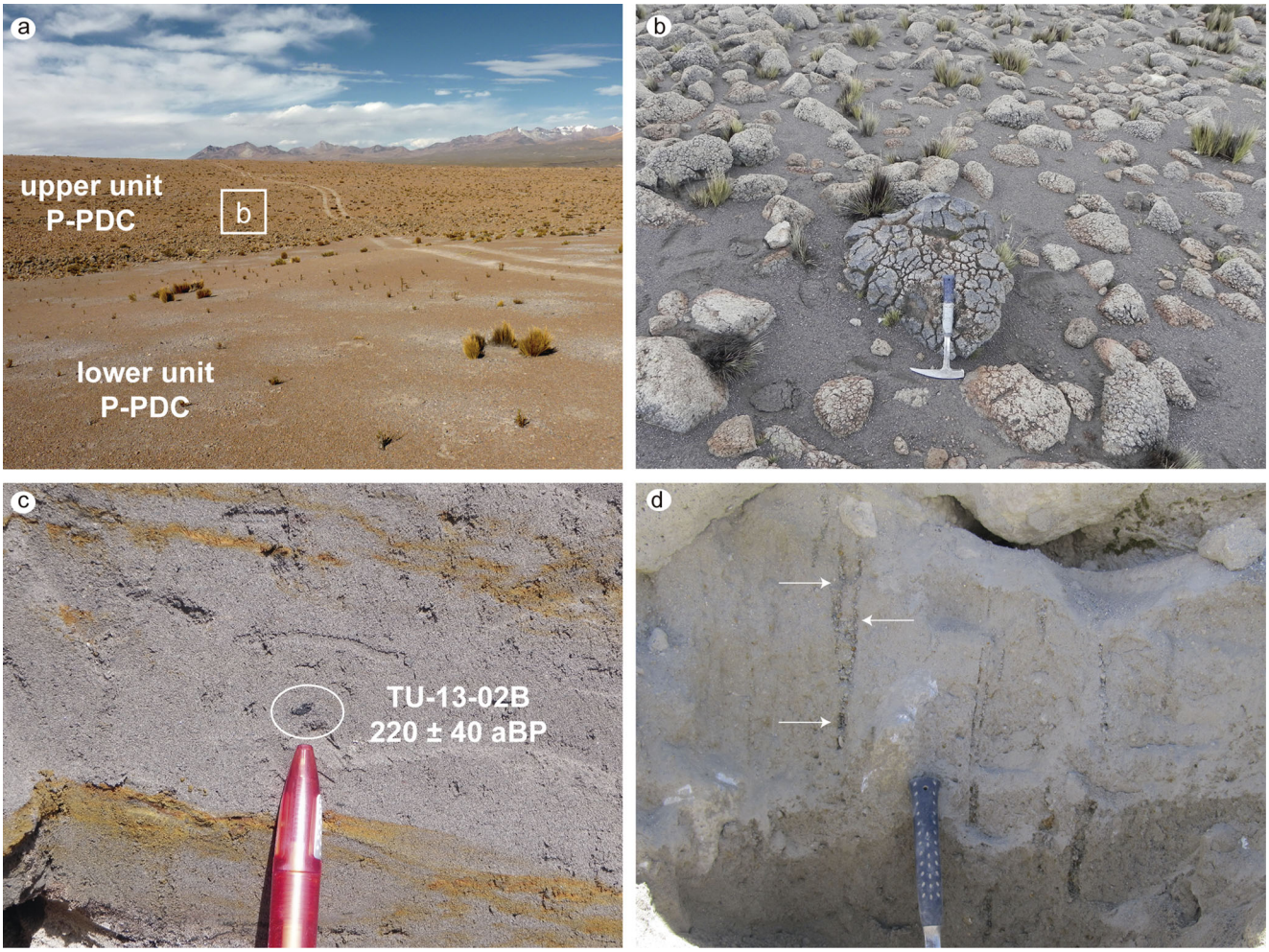

Fig. 7 Paipatja pyroclastic density current deposit (P-PDC). **a** Lower and upper units of P-PDC at Paipatja plain (site 7, Fig. 3). **b** Detail of the upper P-PDC deposit showing the enrichment in decimeter-size cauliflower- and breadcrust-like bombs. **c** Detail of the P-PDC deposit at the Suches lake (site 1, Fig. 3). Note the crude stratification of the fine grained matrix and the presence of many charred twigs and Andean grass (TU-13-02, age indicated). **d** Detail of the P-PDC at the distal end at Callazas valley (site 9, Fig. 3). Note the presence of gas escape pipes (marked by *arrows*)

occasional blocks 0.5–1 m in diameter are also observed. Bombs vary from 10 to 50 cm in size, and they are mostly observed at the deposit's surface. The deposit exhibits slight normal grading overall. No clear differences in the amount of blocks and bombs are observed between the proximal and distal parts of the deposit. In contrast, a progressive decrease in block size is observed with distance.

Extensive exposures of P-PDC unit exist in the Callazas valley, which hosts the maximum deposit runout (sites 9 and 10 at 8–10 km from the amphitheatre, Figs. 3 and 4). There, the P-PDC unit rests on a volcano-sedimentary sequence that includes debris flow deposits and fine-grained lacustrine deposits. The P-PDC deposit is composed of two main layers. The lower layer is mostly ash-rich, whereas the upper layer is highly enriched in bombs at the top of the deposit, with many centimetre-size gas escape pipes. Debris flow deposits comprising reworked material cover the P-PDC unit. Charcoal is extremely scarce in the Paipatja plain deposits, probably because outcrops exposing the base of the deposit are rare. However, at site 10 (Figs. 2 and 3), we found plenty of carbonised grass that yielded an age (235±35 aBP; Table 1), which is radiometrically indistinguishable from those obtained for the Zuripujo PDC deposits (190–230 aBP).

The northern branch of the P-PDC unit outcrops between the Villaque hill and Suches lake (Fig. 2). In this zone, the unit is topographically constrained, 1–2 m thick and appears as a grey, massive layer mostly composed of medium-to-coarse ash with scattered dense lapilli. Its base is composed of a 20–25-cm-thick layer exposing a crude planar stratification with some decimetric lenses of coarser and in places altered (oxidised) material. Overlying this basal layer, the bulk of the deposit does not have any laminations but shows a slight reverse grading. The fact that the P-PDC deposit is exposed in this zone suggests that at least the upper part of the PDC was able to surmount the Villaque hill. In this context, the deposits at Suches lake may have been formed by sedimentation from

the uppermost, more dilute part of the PDC, following the scenario described by Druitt et al. (2002) at Soufrière Hills volcano. The lower part of the unit bears plenty of charred twigs as well as carbonized grass that yield a very similar age to those of the Paipatja plain (i.e. 220±40 aBP; Table 1).

Granulometry and componentry

Grain size analysis was carried out on 14 selected samples from the P-PDC deposit. In the absence of natural, deep cross sections, we sampled the matrix of the deposit by digging (down to 150 cm) in flat areas from the proximal to distal parts of the deposit. Selected grain size histograms (Fig. 8) show that the deposit consists of fine ash to lapilli fragments (−4φ to +5φ), showing a large grain size distribution. Proximal (i.e. sites 11, 10) and central-distal (i.e. sites 12, 13) deposits have similar grain size distributions, which are clearly different from those of lateral deposits (i.e. sites 15C, 02D). In fact, the size distribution of the lateral facies, such as those in the Suches and Zuripujo valleys is almost unimodal, with a fines-enriched trend and good sorting (σ_φ~1-2), whereas central deposits are characterised by a "flat" distribution and poor sorting (σ_φ>2). The P-PDC deposits define a narrower grain size range and tend to be less well sorted than well-known blast deposits (Hoblitt et al. 1981; Druitt 1992; Belousov et al. 2007; Komorowski et al. 2013; Bernard et al. 2014), and fall instead (Fig. 8) into the "pyroclastic flow" field defined by Walker (1983).

Three main types of blocks are observed in the P-PDC deposit, the most abundant being angular to subangular,

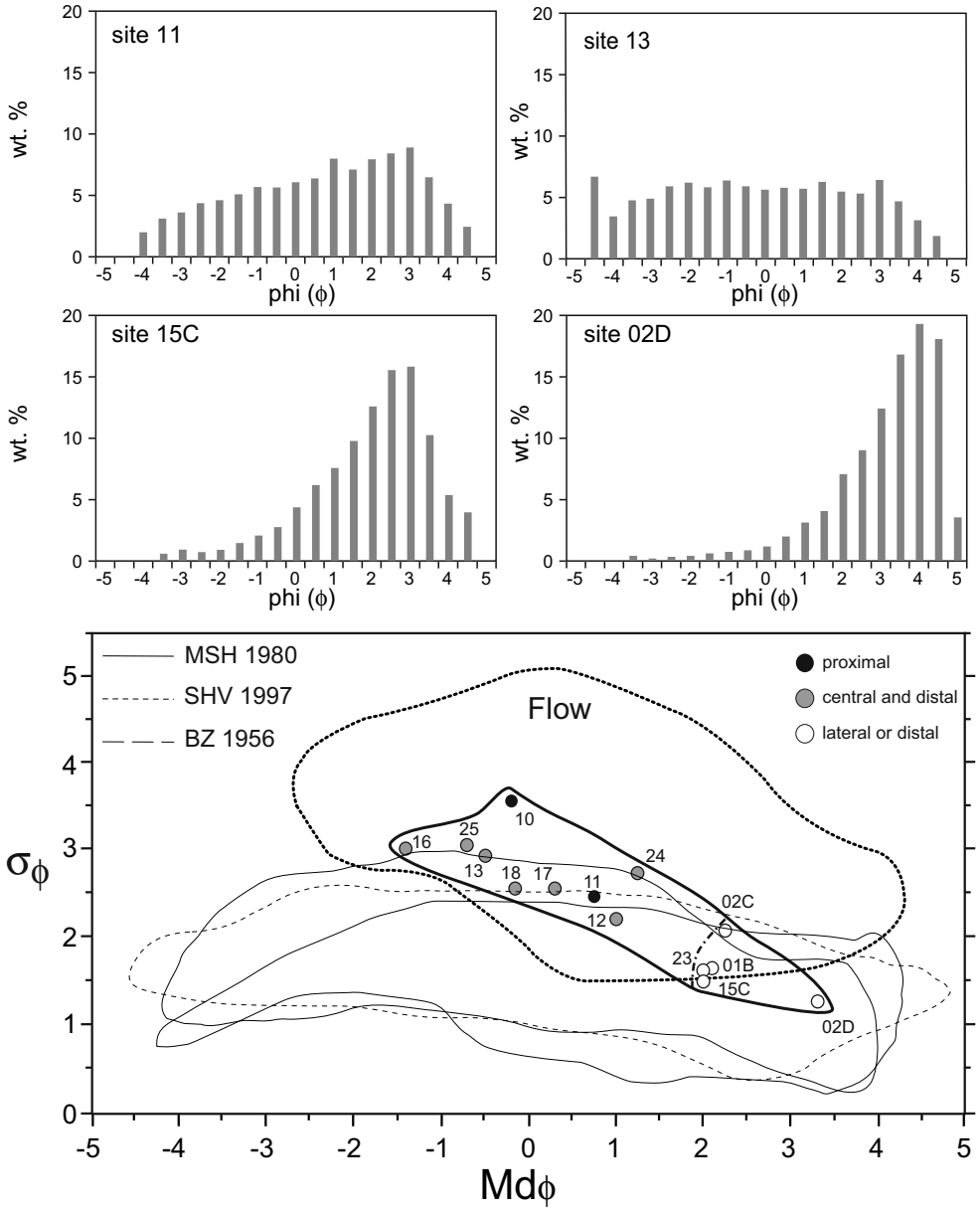

Fig. 8 **a–d** Selected grain size histograms for P-PDC samples. **e** Mdϕ vs σϕ diagram including the "Flow" field (Walker 1983) as well as the fields for different blast deposits (from Belousov et al. 2007). Mount St. Helens (MSH 1980), Bezymianny (BZ 1956) and Soufrière Hills (SHV 1997)

dense, porphyritic dacite blocks with many prismatically jointed fractures. A less abundant component corresponds to vesicular and highly porphyritic cauliflower- and breadcrust-type bombs, which are mostly observed on top of the deposit. A last, minor component corresponds to altered andesitic blocks interpreted as fragments entrained from the basement (*cf.* Roche et al. 2013). For the deposit matrix, we carried out a componentry analysis based on the methodology developed by Eychenne and Le Pennec (2012) in which at least 300 grains were chosen for fractions of −3φ to +1φ. We studied the same 14 samples as for the granulometric analyses, which are distributed from the proximal to distal zones. Three main classes of components were identified: fresh dome fragments, free crystals and altered lava fragments, the latter being interpreted as fragments from the old domes and the basal edifice. Fresh dome fragments range from 57 to 72 wt.%, free crystals (mostly present in the 0φ and +1φ classes) vary from 6 to 18 wt.% and altered fragments range from 20 to 48 wt.%.

Summary of petrologic characteristics

Based on 30 whole-rock major and trace element analyses, the Holocene eruptive products of Tutupaca volcano are classified as high-K calc-alkaline dacites (Fig. 9). All samples from the Eastern Tutupaca domes display a very restricted dacitic composition (64.4–66.1 wt.% SiO_2, normalised to an anhydrous basis, Table 2, Fig. 9), as well as the lava blocks included in the debris avalanche deposits and in the Z-PDC deposits, which show similar chemical characteristics (64.5–65.9 wt.% SiO_2). In contrast, the blocks and bombs of the P-PDC deposits have slightly higher silica contents (65.1–68.0 wt.% SiO_2), especially the scarce pumiceous samples, which have silica-rich compositions (67–68 wt.% SiO_2). For most major and trace elements, Eastern Tutupaca samples lie on the trend defined by the whole Tutupaca volcanic complex (Fig. 9). However, the Eastern Tutupaca rocks display a slight enrichment in some trace elements, namely the light rare earth elements (e.g. La) and a notable depletion in heavy rare earth elements (e.g. Yb), which leads to high La/Yb ratios for these Eastern Tutupaca samples (Fig. 9). A detailed petrological study is in progress, but our current hypothesis is that these characteristics are due to high-pressure crustal processes such as fractionation of amphibole and/or garnet and/or assimilation of deep crustal rocks (*cf.* Thouret et al. 2005; Mamani et al. 2010; Rivera et al. 2014).

Lava samples from the Eastern Tutupaca domes as well as those from the debris avalanche deposit are dark-grey, highly

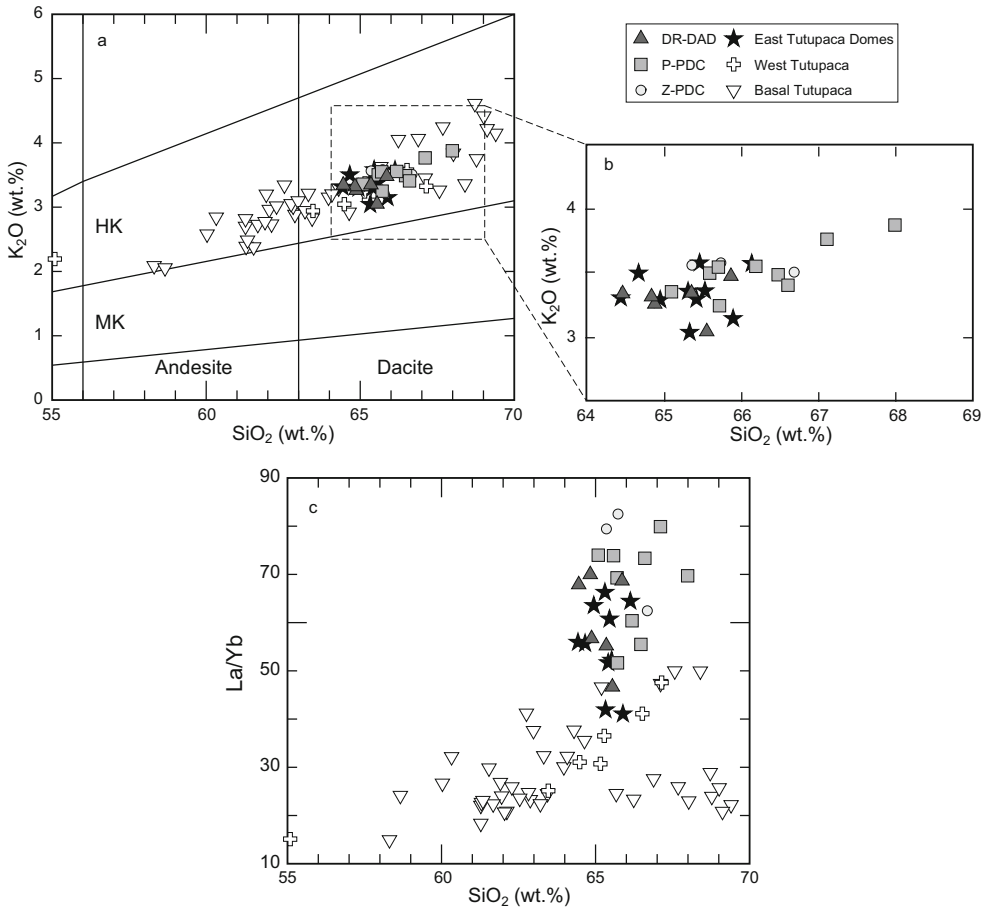

Fig. 9 Selected geochemical data for Tutupaca. **a**, **b** SiO_2 vs K_2O diagram and **c** SiO_2 vs La/Yb

Table 2 Selected whole-rock major (wt.%) and trace element (ppm) analyses of recent Tutupaca eruptive products

Sample no.	TU-12-14	TU-12-18	TU-12-04B	TU-12-09	TU-12-06A	TU-12-06C	TU-12-79A
UTM-Northing	8117106	8116280	8120200	8119422	8119537	8119537	8116684
UTM-Easting	356850	356820	358990	357418	361158	361158	363178
Unit	Recent dome	Recent dome	DR-DAD	HA-DAD	P-PFD	P-PFD	Z-PFD
Description	Lava block	Lava block	Lava block	Lava block	Cauliflower Bomb	Block	Breadcrust bomb
SiO_2 (wt.%)	63.72	64.42	63.39	64.41	64.57	64.06	66.63
TiO_2	0.72	0.72	0.79	0.77	0.70	0.73	0.73
Al_2O_3	15.81	15.80	15.99	15.31	15.56	15.98	15.74
Fe_2O_3*	4.30	4.35	4.40	4.17	4.34	4.35	3.90
MnO	0.06	0.06	0.06	0.06	0.06	0.05	0.05
MgO	1.80	1.61	1.76	1.59	1.64	1.57	1.52
CaO	3.87	3.79	3.91	3.61	3.51	3.76	3.36
Na_2O	4.34	4.30	4.47	4.18	4.15	4.35	4.20
K_2O	3.23	3.32	3.29	3.40	3.49	3.30	3.51
P_2O_5	0.27	0.28	0.30	0.30	0.27	0.27	0.27
LOI	0.21	−0.04	0.23	0.51	0.95	0.17	0.64
TOTAL	98.33	98.61	98.58	98.31	99.24	98.60	100.56
Sc (ppm)	6.55	5.56	6.67	5.79	5.39	5.52	5.37
V	91.00	93.20	92.60	82.70	88.33	90.52	75.33
Cr	11.75	11.62	12.80	9.43	10.94	11.75	10.26
Co	11.71	11.20	11.33	13.99	12.21	10.03	12.30
Ni	11.92	10.66	10.12	7.38	11.18	9.79	6.74
Rb	104.68	104.11	97.83	102.77	109.82	102.35	115.51
Sr	764.15	763.48	836.36	774.71	716.60	798.88	714.95
Y	8.21	8.30	9.06	8.85	7.37	7.88	8.73
Zr	128.04	138.62	148.80	134.70	134.36	134.31	143.19
Nb	7.50	7.78	8.51	8.97	6.82	8.26	8.83
Ba	1289.39	1309.65	1275.39	1334.10	1235.74	1320.77	1324.95
La	35.74	37.32	39.54	40.57	35.46	37.32	38.71
Ce	69.20	70.62	78.71	79.53	67.32	69.97	94.22
Nd	27.80	28.60	31.78	32.05	26.29	28.67	30.23
Sm	4.73	5.54	5.99	5.21	4.16	4.96	5.23
Eu	1.09	1.13	1.31	1.32	1.15	1.28	1.24
Gd	3.16	3.10	3.46	3.58	3.07	2.99	3.58
Dy	1.81	1.88	2.00	1.82	1.57	1.65	2.03
Er	0.65	0.58	0.71	−0.03	0.61	0.47	0.95
Yb	0.56	0.56	0.58	0.59	0.51	0.50	0.62
Th	8.30	8.41	8.28	9.73	9.10	8.03	9.90

Analyses were performed at the Laboratoire des Domaines Océaniques, Université de Bretagne Occidentale, Brest (France), by ICP-AES, except Rb, performed by flame atomic emission spectrometry, following the procedure of Cotten et al. (1995). Relative standard deviations are <2 and 5 % for major and trace elements, respectively

LOI loss on ignition

*Total iron as Fe_2O_3

porphyritic (30–40 vol.%) dacites containing plagioclase (10–20 vol.%), amphibole (10 vol.%), biotite (5 vol.%) and Fe-Ti oxides (2–3 vol.%). We also found ortho- and clinopyroxene, sphene, quartz and apatite as accessory phases (≤1 vol.%). Two populations of plagioclase were observed, the main group corresponding to euhedral, fresh, zoned phenocrysts (up to 4 mm), and the subordinate group (<3–4 vol.%) consisting of subhedral crystals with frequent disequilibrium textures such as reaction rims and dusty concentric zones and cores. The second most abundant mineral is amphibole, which appears as fresh, euhedral crystals (<1 mm) or is partially to completely replaced by a microcrystalline assemblage

composed of oxides (opacite). Biotite, which appears as euhedral to subhedral phenocrysts (up to 1–2 mm), represents the third main phase, frequently showing intergrowth textures with amphibole, plagioclase and Fe-Ti oxides. These phases, together with the other accessory minerals, are included in a vitreous to intersertal groundmass with a maximum of 5–10 vol.% vesicles. The dense blocks from the P-PDC deposit have a texture and a mineral assemblage similar to that of the lava dome blocks described above. In contrast, the bombs are more vesiculated (up to 40 vol.%) and display a high crystallinity (15–20 vol.% phenocryst) and the same mineral assemblage as the dense blocks. In conclusion, the geochemical and petrographical characteristics are useful tools to discriminate Eastern Tutupaca eruptive products from older products of Western and Basal Tutupaca edifices. We stress the strong homogeneity of the recent Tutupaca dacites and the fact that the young domes, the blocks from the DA deposit (namely those from the DR-DAD), and the juvenile samples from the P-PDC deposit share the same geochemical and petrographical characteristics.

Discussion

Historic chronicles and age of the Tutupaca sector collapse

Historical chronicles reported by Fidel and Zavala (2001) clearly point to an explosive eruption of Tutupaca volcano during the last few centuries. Zamacola y Jaúregui (1804) describes that "*now 15 years* (i.e. around 1789 AD) *burst* (a volcano) *close to the village of Candarave, distant 60 leagues from this city (*i.e. Arequipa; 1 Castellan league is about 4.2 kilometres)*, since that time, it has been smoking incessantly; but there will be two years* (i.e. in 1802 AD), (the volcano) *made a formidable explosion that its ashes and noise reached more than 100 leagues*" (this text and the next one were translated by the authors from the original texts in Spanish). Valdivia (1847) is more explicit since he mentions that "*on March, 20 1802 burst Tutupaca, leaving for five months ash in the air, (and) getting dark the atmosphere as far as Locumba, Tacna and Arica* (cities located in the south-western coastal zone)". These chronicles are corroborated by the oral tradition of the Candarave inhabitants, who consider Tutupaca as "the villain", in comparison to the "the good" Yucamane. This perception seems clearly related to the past explosive eruptions of Tutupaca and their impacts on local communities (Zora Carvajal 1954). These chronicles clearly show that Tutupaca experienced a strong explosive episode that started around 1787 AD and whose paroxysm probably occurred in 1802 AD.

The historic information is corroborated by the five radiocarbon ages (Table 1) we obtained from charcoal samples from the Z-PDC deposit in the Zuripujo valley and the P-PDC deposit on the Paipatja plain and nearby Suches lake. Samples from the Z-PDC deposit yield two well-constrained ages (220±30 and 230±30 aBP, Table 1), and a third slightly younger one (190±30 aBP), whereas the two samples from the P-PDC deposits give very close ages (220±40 and 235±35 aBP, Table 1). We calibrated these conventional ^{14}C ages to calendar ages using the Calib 6.0 code (Stuiver and Reimer 1993; Stuiver et al. 2005) and the Southern Hemisphere calibration curve (SHCal04, McCormac et al. 2004), which is suitable for this region and is available back to 11 ka cal BP (Fig. 10). Results of this calibration procedure show that the five samples are statistically identical at a 95 % confidence level with a pooled mean of 218±14 aBP. The calibrated calendar age for this average ^{14}C age yields two age spans, the most important being 1731–1802 cal AD period (with a relative area of 85 %). We emphasise that the two historic eruptions (1787–89 and 1802 AD) reported by Zamácola y Jaúregui (1804) and Valdivia (1847) fall at the end of this period.

Unfortunately, radiocarbon data are unable to discriminate between the pre-collapse flows (i.e. the Zuripujo event) and the syn-collapse pyroclastic event (i.e. Paipatja event). However, the stratigraphic evidence unambiguously shows that the Zuripujo event (Z-PDC) preceded the sector collapse and the associated explosive phase (DAD and P-PDC). Thus, we can state that the time between these two volcanic events was too short to be resolved using the radiocarbon method (i.e. some years to a few decades).

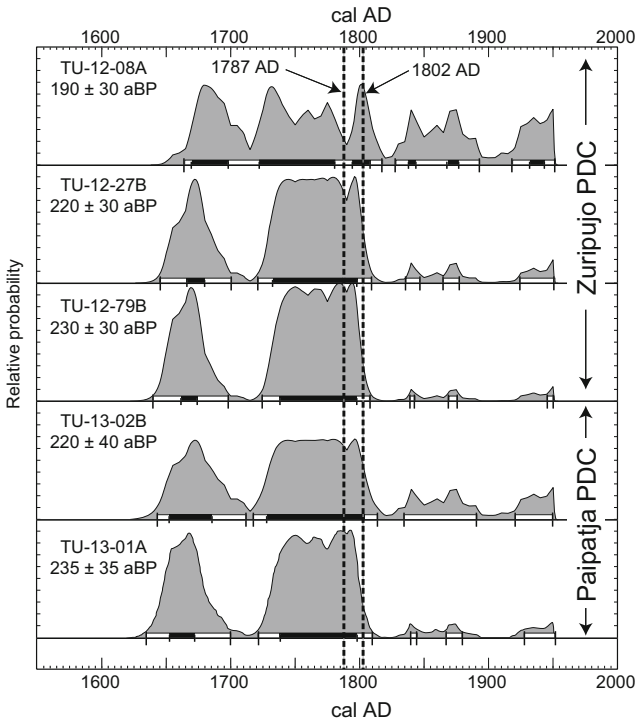

Fig. 10 Density probability functions for the calibrated radiocarbon ages of the last Tutupaca explosive eruption

Magnitude of the explosive phase

With the aim of estimating the magnitude of the explosive phase accompanying the debris avalanche of Tutupaca, we estimated the volume of the Paipatja pyroclastic density current (P-PDC) deposit. Satellite image inspection, coupled with detailed fieldwork including almost 300 GPS points, led to the establishment of a detailed map and made it possible to constrain the whole area covered by the P-PDC deposits (Fig. 3). In addition, we also mapped the mostly reworked, distal and lateral deposits of the P-PDC, which are interpreted as the related derived ash-cloud surge deposit. As a result, the main unit of the P-PDC covers an area of ~35–40 km^2, whereas the distal and lateral deposits have a larger distribution, covering an area of ~100–105 km^2. Last, in absence of natural, deep cross sections, we estimated an average thickness by digging in flat areas representative of the different parts of the deposit (75 holes for the whole P-PDC unit). On the Paipatja plain we found an average thickness of ~0.5-1 m, whereas in the valleys descending to the Rio Callazas, we observed a thickness range of 2–5 m. Based on these estimates, we obtained a volume of ~$5–6\times10^7$ m^3 for the main P-PDC deposit. For deposits of the uppermost ash-cloud layer, we estimate an average thickness of 15 cm and obtain a volume of ~1.5×10^7 m^3. Thus, the total bulk volume for the P-PDC is of the order of ~$6.5–7.5\times10^7$ m^3, corresponding to a VEI 3 eruption. We did not find proximal tephra fallout deposits associated with this eruption. Historical chronicles, however, suggest that distal fine ash fallout occurred in the coastal region at Locumba (77 km to the SW of Tutupaca), Tacna (110 km to the S) and Arica (165 km to the S). Because we have no constraints on the extent of these distal fine ash fallout deposits, the total eruption volume is underestimated. Considering such uncertainties, the bulk volume was probably greater than that calculated for the preserved deposits, implying that the eruption might well rank as a VEI 4. In summary, this eruption probably represents the youngest debris avalanche in the Andes and was accompanied by one of the larger explosive events in Peru during historical times.

Eruptive dynamics of the pyroclastic density currents

Explosive eruptive activity frequently accompanies sectorial collapse of volcanic edifices, especially in the case of violent decompression of a shallow magma body (see Belousov et al. 2007, for review and references therein). As a result, the explosive eruption produces so-called lateral or directed blast-generated pyroclastic density currents. Thus, blast deposits are intimately associated with debris avalanche deposits. This association formed during the recent eruptions of Bezymianny in 1956 (Belousov 1996), Mount St. Helens in 1980 (Hoblitt et al. 1981) and Soufrière Hills, Monserrat in 1997 (Voight et al. 2002). It is important to note that at Bezymianny and Mount St. Helens, the source of the explosion was a cryptodome that triggered the flank failure, whereas at Soufrière Hills, Monserrat, the source of the explosion was a growing lava dome. A similar scenario was described by Macías et al. (2010) at Tacaná volcano (southern México). In this case, however, the debris avalanche was associated with block-and-ash flows without a blast.

Explosive events also occur when the magma reservoir is too deep to produce a lateral blast. In these cases, decompression of the upper part of the magmatic system triggers a sustained plinian eruption and related pumice-rich pyroclastic flows. This occurred during the 1964 eruption of Shiveluch volcano (Belousov et al. 1999). In this case, a time delay exists between the sector collapse and the subsequent explosive activity. As a result, the contact between the debris avalanche deposits and the covering pyroclastic deposits is well-defined.

Lateral explosions producing similar blast-generated pyroclastic density currents are also associated with growing lava domes with no sector collapse. This occurred during the well-known eruption of Montagne Pelée, Martinique in 1902 (Bourdier et al. 1989), and recently during the 2010 Merapi eruption (Komorowski et al. 2013). This scenario also occurred during the explosive destruction of a lava dome at Chachimbiro volcanic complex, Ecuador (Bernard et al. 2014). In these cases, the growing lava dome exploded as a result of a high extrusion rate, which prevented efficient outgassing. It is also important to note that, in these examples, no associated debris avalanche deposits have been described.

In the case of the Tutupaca sector collapse, there is no plinian fallout deposit associated with the debris avalanche and the pyroclastic density current deposits. However, several pieces of evidence suggest that magmatic activity was intimately linked with the sector collapse. These include the intimate stratigraphic relations between the DA deposit and the P-PDC deposits, the fact that the P-PDC deposits cover a sector whose angle coincides with the that of the DA deposit (Fig. 11), the presence of prismatically jointed blocks in the DR-DAD, and the petrological similarity between the juvenile clasts in the DA, the P-PDC deposits and the recent Tutupaca domes. Figure 11 depicts the deposit of the lateral blasts that accompanied the Bezymianny, Mount St. Helens, and Soufrière Hills (Monserrat) sector collapses. At Tutupaca, the PDC deposits cover an area similar to that at Soufriere Hills, Montserrat, in agreement with the estimated bulk volumes (8×10^7 m^3 for Tutupaca, and 3×10^7 m^3 for Montserrat, Belousov et al. 2007). We also observe a similarity between Tutupaca and Mount St. Helens in terms of the blast propagation angle and the digitate shape of the devastation zone. This last feature, however, is probably related to the fact that the Mount St. Helens blast deposit was mapped in greater detail compared with the Bezymianny and Soufrière Hills blast deposits (note that the latter extend into the sea in distal areas). However, the sedimentological characteristics of the P-PDC

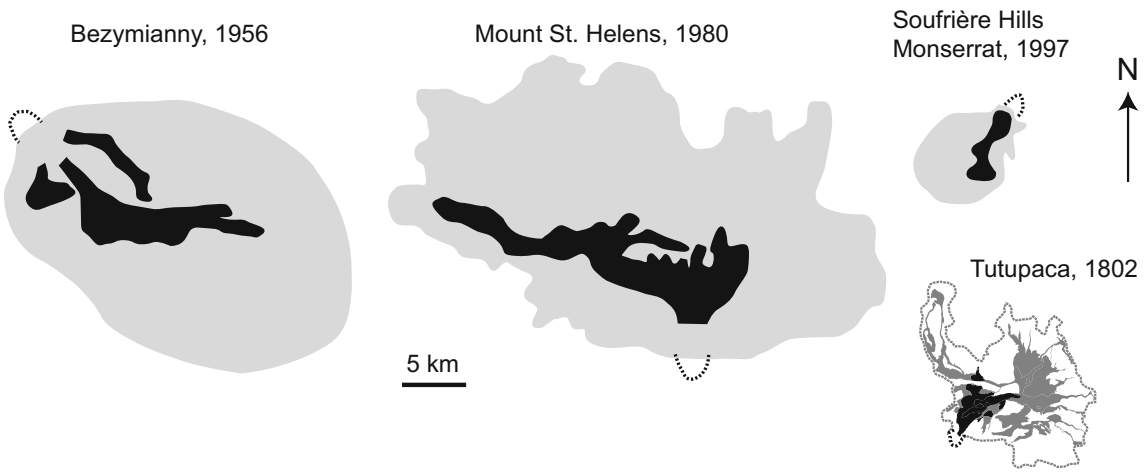

Fig. 11 Distribution of the blast deposits (*grey*) associated with well-known debris avalanches (*black*). *Dotted lines* represent the amphitheatre. Modified from Belousov et al. (2007)

deposit do not match those of the above-mentioned blast deposits as reported by Belousov et al. (2007). These authors report that blast deposits are characterised by three distinct units: (i) a basal layer with evidence of material entrainment from the substrate, (ii) a thicker, middle layer that is fines-depleted, normally graded and well sorted, and (iii) an upper, fines-rich layer with frequent planar and wavy laminations. This three-layer sequence may reflect emplacement of a dilute, turbulent and erosive current with a possible lower layer of higher particle concentration. The P-PDC deposits associated with the Tutupaca debris avalanche do not show the deposit sequence identified by Belousov et al. (2007). Instead, the field observation and the sedimentological characteristics suggest a fairly concentrated basal flow (Fig. 8) with an associated dilute cloud that was able to overpass topographic barriers (for instance the Villaque hill). Thus, we propose that the P-PDC deposits result from pyroclastic density currents formed during a lateral eruption by asymmetrical fountain collapse associated with the Tutupaca sector collapse. A last point to be stressed is that after the sector collapse and its associated pyroclastic density currents, no magmatic activity occurred at Tutupaca. This fact is in sharp contrast with what has been described at other volcanoes that experienced sector collapses (such as Bezymianny, Mount St. Helens or Soufriere Hills).

Reconstruction of the eruptive events

The Eastern Tutupaca dome complex consists of at least 7 coalesced dacitic domes that grew during Holocene times on top of an old, hydrothermally altered basal edifice (Manrique 2013). This dome complex was active in the late 18th century and was affected, between 1787 and 1802 AD, by a major sector collapse that produced a debris avalanche and the associated pyroclastic density currents whose deposits are described in this manuscript. This event was preceded by the block-and-ash flows whose deposits outcrop in the Zuripujo valley to the SE of the Eastern Tutupaca summit (the Z-PDC deposits). These deposits have a limited lateral extent, and mostly outcrop in an almost orthogonal position with respect to the NE-opening amphitheatre, which may reflect a focused flow direction from the source area. In addition, the Z-PDC deposits are overlain by a partially reworked ash-rich layer that represents the lateral facies of the later Paipatja pyroclastic density current deposits (P-PDC, Fig. 5). On the basis of these constraints, we propose that the Z-PDC represents a volcanic event that preceded the Tutupaca sector collapse. This inference is also supported by the fact that charcoal fragments are abundant in the Z-PDC deposits but are extremely rare in the P-PDC deposits, which suggests that the Z-PDC charred and covered the rare vegetation (mainly grass and small bushes) of this high Andean plateau. An additional point to be taken into consideration concerns the fact that the Z-PDC deposit contains a large amount of altered (hydrothermal) components, which contrasts with the rather scarce juvenile material that has been observed in the P-PDC. Thus, the Z-PDC was probably associated with vent clearing explosions occurring in a pressurised lava dome and its subsequent collapse along a sliding plane that was deep enough in the dome to significantly affect the hydrothermal system. As a result, parts of the dome with large amounts of hydrothermally altered material collapsed, producing the pyroclastic flow deposits of the Zuripujo valley. This type of activity has been described at other andesitic and dacitic domes such as Galeras, Colombia (Calvache and Williams 1992) and Soufrière Hills, Monserrat (Sparks et al. 2002).

Dome growth activity proceeded on the Eastern Tutupaca edifice and culminated with the sector collapse that affected its NE flank, following a scenario that was described for the 1997 sector collapse of Soufrière Hills, Monserrat (Sparks et al. 2002) as well as at Tacaná volcano, México (Macías et al.

2010). In the case of Tutupaca, the sector collapse affected the dome complex and the hydrothermally altered lavas of the basal edifice. As a result, a relatively small (<1 km^3) debris avalanche spread at the foot of the amphitheatre and reached the Paipatja plain 6–8 km away. The debris avalanche had two main units. The first unit is mainly composed of hydrothermally altered rocks (HA-DAD) from the basal edifice, although it also includes non-altered dome blocks. This lower unit (Unit 1 in Valderrama et al. 2014) is the more voluminous and shows morphological features such as megablocks and hummocks. The upper part of this unit indicates a different dynamical behaviour, expressed by the presence of surface ridges (Unit 2a of Valderrama et al. 2014). The second unit (DR-DAD) also displays frequent surface ridges (Unit 2b of Valderrama et al. 2014), covers the previous one and comprises unaltered dacitic blocks with frequent prismatically jointed blocks, which attest to thermal contraction. This suggests that the second debris avalanche pulse was associated with the collapse of an active dome complex located at the former Tutupaca summit.

In between these debris avalanche units, the voluminous ($6.5–7.5\times10^7$ m^3) Paipatja pyroclastic density current deposit (P-PDC) extends up to 10–12 km down the Callazas river (to the NE) and the Suches lake (to the N). This pyroclastic sequence overlies the HA-DAD and is interstratified with (or covered by) the DR-DAD, which shows that the debris avalanche and the pyroclastic flows were generated quasi-synchronously.

Comparison with other debris avalanche deposits in the Central Andes

Based on satellite image analysis, Francis and Wells (1988) published an inventory of the most prominent debris avalanche deposits in the Central Andes. Since then, many detailed field-based studies have been focused on these deposits, which rank among the most spectacular debris avalanches on earth. Examples include the debris avalanche deposits of Socompa (van Wyk de Vries et al. 2001; Kelfoun et al. 2008), Parinacota (Clavero et al. 2002), Tata Sabaya (de Silva et al. 1993), Ollagüe (Clavero et al. 2004) and Llullaillaco (Richards and Villeneuve 2001). Compared with these examples, the Tutupaca debris avalanche differs in its small areal coverage (12–13 km^2) and volume (<1 km^3); its area is one order of magnitude smaller that the huge surfaces covered by the Socompa (490 km^2), Tata Sabaya (~300 km^2), Parinacota (140 km^2), Ollagüe (~100 km^2) or Llullaillaco (165 km^2) debris avalanche deposits. In spite of its modest size, the Tutupaca debris avalanche deposit is important for two main reasons. First, because at Tutupaca, the debris avalanche deposits are intimately associated with a sequence of pyroclastic density current deposits, pointing clearly to a magmatic origin for the sector collapse. Second, due to its young age and high degree of preservation, Tutupaca is a unique place for studying the origin and implications of the elongate ridges that characterise this deposit (cf. Valderrama et al. 2014).

Conclusions

The younger (Eastern) edifice of the Tutupaca volcanic complex is a Late Holocene dacitic dome complex that was affected by a sector collapse in historical times. The collapse triggered a small (<1 km^3) debris avalanche and associated pyroclastic density currents whose deposits have a bulk volume of about $6.5–7.5\times10^7$ m^3, which ranks this eruption as at least a VEI 3 event. Both deposits, of the avalanche and the pyroclastic density currents, were emplaced synchronously and spread onto the plain NE of Tutupaca volcano. The ^{14}C age determinations obtained for the pyroclastic flow deposits yield a mean age of 218±14 aBP, which corresponds to an eruption that occurred in the 18th century (1731–1802 cal AD). This age is in agreement with the historical chronicles that report major explosive activity at Tutupaca in the period between 1787 and 1802 AD.

The spatial and temporal relationships between deposits of the debris avalanche and the Paipatja pyroclastic density currents (P-PDC), coupled with the petrological similarity between the juvenile fragments in both deposits, indicate that juvenile magma was involved in the sector collapse. A pressurised dome complex triggered the first pyroclastic density currents (Z-PDC). Then, ascent of a dacitic magma batch, coupled with the fact that the Tutupaca dome complex was constructed on top of a highly altered and hydrothermally active volcanic system, triggered the destabilisation of the edifice, producing the debris avalanche and its related pyroclastic density currents represented by the P-PDC.

On the basis of our work on the most recent eruption at Tutupaca, a future eruption of this volcano may display similar eruptive dynamics characterised by viscous dome growth and related block-and-ash pyroclastic flows. This scenario is corroborated by the pre-historical activity of Tutupaca, which shows a frequent pattern of dome growth and collapse as well as at least one other, older debris avalanche event. During the past eruptions of Tutupaca, the eruptive products affected uninhabited areas of the high Andes in Peru, and tephra fallout had only a minor regional impact. However, if a large eruption occurred today, it could affect a much larger population of at least eight to ten thousand inhabitants living within a 25-km radius of the volcano, as well as the important mining (Toquepala, Cuajone) and geothermal (Calientes) infrastructures located in the proximity of Tutupaca.

Acknowledgments This work is part of a Peruvian–French cooperation programme carried out between the Instituto Geológico, Minero y Metalúrgico (INGEMMET, Peru) and the Institut de Recherche pour le Développement (IRD, France). It was partially founded by a "Jeunes Equipes Associées à l'IRD" (JEAI) project that is an initiative designed to promote and strengthen new research teams in developing countries. We warmly thank Etienne Medard, Pierre Delmelle, Marie Detienne, Karine Bernard, Marco Rivera and Jean-Luc Le Pennec for fruitful discussions on the field and Fran van Wyk des Vries for the english improvement of the manuscript. We are grateful to the two anonymous reviewers for their comments and with S. De la Cruz-Reyna and J.D.L. White for the editorial handling. This research was financed by the French Government Laboratory of Excellence initiative no. ANR-10-LABX-0006, the Région Auvergne and the European Regional Development Fund. This is Laboratory of Excellence ClerVolc contribution no. 159.

References

Adams NK, de Silva SL, Self S, Salas G, Schubring S, Permenter JL, Arbesman K (2001) The physical volcanology of the 1600 eruption of Huaynaputina, southern Peru. Bull Volcanol 62:493–518

Belousov A (1996) Pyroclastic deposits of March 30, 1956 directed blast at Bezymianny volcano. Bull Volcanol 57:649–662

Belousov A, Belousova M, Voight B (1999) Multiple edifice failures, debris avalanches and associated eruptions in the Holocene history of Shiveluch volcano, Kamchatka, Russia. Bull Volcanol 61:324–342

Belousov A, Voight B, Belousova M (2007) Directed blasts and blast-generated pyroclastic density currents: a comparison of the Bezymianny 1956, Mount St. Helens 1980, and Soufrière Hills, Montserrat 1997 eruptions and deposits. Bull Volcanol 69:701–740

Benavente C, Carlotto V, del Castillo B (2010) Extensión en el arco volcánico actual del Sur de Perú. XV Congreso Peruano de Geología, Extended abstracts. Sociedad Geológica del Perú, Lima

Bernard B, Hidalgo S, Robin C, Beate B, Quijozaca J (2014) The 3640–3510 BC rhyodacite eruption of Chachimbiro compound volcano, Ecuador: a violent directed blast produced by a satellite dome. Bull Volcanol 76:849. doi:10.1007/s00445-014-0849-z

Bourdier JL, Boudon G, Gourgaud A (1989) Stratigraphy of the 1902 and 1929 nude ardente deposits, Mt. Pelée Martinique. J Volcanol Geotherm Res 38:77–96

Bromley GRM, Schaefer JM, Wincler G, Hall BL, Todd CE, Rademaker CKM (2009) Relative timing of last glacial maximum and late-glacial events in the central tropical Andes. Quat Sci Rev 28: 2514–2526

Calvache ML, Williams SN (1992) Lithic-dominated pyroclastic flows at Galeras volcano, Colombia – an unrecognized volcanic hazard. Geology 20:539–542

Clavero JE, Sparks RSJ, Huppert HE, Dade WB (2002) Geological constraints on the emplacement mechanism of the Parinacota debris avalanche, Northern Chile. Bull Volcanol 64:40–54

Clavero JE, Polanco E, Godoy E, Aguilar G, Sparks S, van Wyk de Vries B, Pérez de Arce C, Matthews S (2004) Substrata influence in the transport and emplacement mechanisms of the Ollagüe debris avalanche, Northern Chile. Acta Vulcanol 16:59–76

Cobeñas G, Thouret JC, Bonadonna C, Boivin P (2012) The c.2030 yr BP Plinian erup- tion of El Misti volcano, Peru: eruption dynamics and hazard implications. J Volcanol Geotherm Res 241–242:105–120

Cotten J, Le Dez A, Bau M, Caroff M, Maury RC, Dulski P, Fourcade S, Bohn M, Brousse R (1995) Origin of anomalous rare-earth element and Yttrium enrichments in subaerial exposed basalts: evidence from French Polynesia. Chem Geol 119:115–138

de Silva SL, Francis P (1990) Potentially active volcanoes of Peru: observations using Landsat Thematic Mapper and space shuttle photography. Bull Volcanol 52:286–301

de Silva SL, Davidson JP, Croudace IW, Escobar A (1993) Volcanological and petrological evolution of Volcan Tata Sabaya, SW Bolivia. J Volcanol Geotherm Res 55:305–335

Druitt TH (1992) Emplacement of the 18 May 1980 lateral blast deposit ENE of Mount St. Helens, Washington. Bull Volcanol 54:554–573

Druitt TH, Calder ES, Cole PD, Hoblitt RP, Loughlin SC, Norton GE, Ritchie LJ, Sparks RSJ, Voight B (2002) Small-volume, highly mobile pyroclastic flows formed by rapid sedimentation from pyroclastic surges at Soufrière Hills Volvano, Monserrat: an important volcanic hazard. In: Druitt T, Kokelaar BP (eds), The eruption of Soufrière Hills Volcano, Montserrat, from 1995 to 1999. Mem Geol Soc London 21: 263–279

Eychenne J, Le Pennec JL (2012) Sigmoidal particle density distribution in a subplinian scoria fall deposit. Bull Volcanol 74:2243–2249. doi:10.1007/s00445-012-0671-4

Fidel L, Zavala B (2001) Mapa preliminar de amenaza volcánica del volcán Tutupaca. Boletín 24, Serie C: Geodinámica e Ingeniería Geológica, INGEMMET, 109 p

Francis PW, Wells GL (1988) Landsat Thematic Mapper observations of debris avalanche deposits in the Central Andes. Bull Volcanol 50: 258–278

Gerbe MC, Thouret JC (2004) Role of magma mixing in the petrogenesis of lavas erupted through the 1990–98 explosive activity of Nevado Sabancaya in south Peru. Bull Volcanol 66:541–561

Glicken H (1991) Sedimentary architecture of large volcanic-debris avalanches. Sedimentation in Volcanic Settings. SEPM Spec Publ 45: 99–106

Hantke G, Parodi A (1966) Catalogue of the active volcanoes of the world, Part XIX, Colombia, Ecuador and Peru, IAVCEI Naples, Italy, 73 pp

Harpel CJ, de Silva S, Salas G (2011) The 2 ka eruption of Misti Volcano, Southern Peru—the most recent plinian eruption of arequipa's iconic volcano. Geol Soc Am Spec Pap 484:1–72. doi:10.1130/2011.2484

Hoblitt RP, Miller CD, Vallance JW (1981) Origin and stratigraphy of the deposit produced by the May 18 directed blast. In: Lipman PW, Mullineaux DR (eds) The 1980 eruptions of Mount St. Helens, Washington. USGS Prof Paper 1250:401–419

Kelfoun K, Druitt TH, van Wyk de Vries B, Guilbaud MN (2008) Topographic reflection of the Socompa debris avalanche, Chile. Bull Volcanol 70:1169–1187

Komorowski JC, Jenkins S, Baxter PJ, Picquout A, Lavigne F, Charbonnier S, Gertisser R, Preece K, Cholik N, Budi-Santoso A, Surono (2013) Paroxysmal dome explosion during the Merapi 2010 eruption: processes and facies relationships of associated high- energy pyroclastic density currents. J Volcanol Geotherm Res 261: 260–294. doi:10.1016/j.jvolgeores.2013.01.007

Macías JL, Arce JL, García-Palomo A, Mora JC, Layer PW, Espíndola JM (2010) Late-Pleistocene flank collapse triggered by dome growth at Tacaná volcano, México-Guatemala, and its relationship to the regional stress regime. Bull Volcanol 72:33–53. doi:10.1007/s00445-009-0303-9

Mamani M, Worner G, Sempere T (2010) Geochemical variations in igneous rocks of the Central Andean orocline (13°S to 18°S): tracing crustal thickening and magma generation through time and space. Geol Soc Am Bull 122:162–182

Manrique N (2013) Evolución Vulcanológica y Magmática del Edificio Reciente del Complejo Volcánico Tutupaca (Tacna). Universidad Nacional San Agustín de Arequipa. Tesis. 90 p

McCormac FG, Hogg AG, Blackwell PG, Buck CE, Higham TFG, Reimer PJ (2004) SHCal04 Southern Hemisphere Calibration 0–11.0 cal Kyr BP. Radiocarbon 46:1087–1092

Richards JP, Villeneuve M (2001) The Llullaillaco volcano, northwest Argentina: construction by Pleistocene volcanism and destruction by sector collapse. J Volcanol Geotherm Res 105:77–105

Rivera M, Thouret JC, Samaniego P, Le Pennec JL (2014) The 2006–2009 activity of Ubinas volcano (Peru): petrology of the 2006 eruptive products and insights into genesis of andesite magmas, magma recharge and plumbing system. J Volcanol Geotherm Res 270:122–141

Roche O, Niño Y, Mangeney A, Brandt B, Pollock N, Valentine GA (2013) Dynamic pore-pressure variations induce substrate erosion by pyroclastic flows. Geology 41:1107–1110

Siebert L, Simkin T, Kimberly P (2010) Volcanoes of the world. Third edition. Smithsonian Institution and University of California press. 551 p

Smith JA, Mark BG, Rodbell DT (2008) The timing and magnitude of mountain glaciation in the tropical Andes. J Quat Sci 23:609–634

Sparks RSJ, Barclay J, Calder ES, Herd RA, Luckett R, Norton GE, Pollard L, Robertson RA, Ritchie L, Voight B, Young SR, Woods AW (2002) Generation of a debris avalanche and violent pyroclastic density current: the Boxing Day eruption of 26 December 1997 at the Soufrière Hills volcano, Montserrat. In: Druitt T, Kokelaar BP (eds) The eruption of Soufrière Hills volcano, Montserrat, from 1995–1999. Mem Geol Soc London 21:409–434

Stuiver M, Reimer PJ (1993) Extended 14C database and revised CALIB radiocarbon calibration program. Radiocarbon 35:215–230

Stuiver M, Reimer PJ, Reimer RW (2005) CALIB 5.0. [WWW program and documentation]

Thouret JC, Davila J, Eissen JP (1999) Largest historic explosive eruption in the Andes at Huaynaputina volcano, south Peru. Geology 27: 435–438

Thouret JC, Finizola A, Fornari M, Suni J, Legeley-Padovani A, Frechen M (2001) Geology of El Misti volcano nearby the city of Arequipa, Peru. Geol Soc Am Bull 113:1593–1610

Thouret JC, Rivera M, Wörner G, Gerbe MC, Finizola A, Fornari M, Gonzales K (2005) Ubinas: the evolution of the historically most active volcano in southern Peru. Bull Volcanol 67:557–589

Valderrama P, Roche O, Samaniego P, van Wyk des Vries B, Bernard K (2014) The dynamic implications of ridged textures on a volcanic debris avalanche deposit at Tutupaca volcano, Southern Peru. Submitted to Geology (April 2015)

Valdivia JG (1847) Fragmentos para la historia de Arequipa. Folletín de "El Deber", Arequipa, 109–111 p

van Wyk de Vries B, Self S, Francis PW, Keszthelyi L (2001) A gravitational spreading origin for the Socompa debris avalanche. J Volcanol Geotherm Res 105:225–247

Voight B, Komorowski JC, Norton GE, Belousov AB, Belousova M, Boudon G, Francis PW, Franz W, Heinrich P, Sparks RSJ, Young SR (2002) The 1997 Boxing Day Sector Collapse and Debris Avalanche, Soufriere Hills Volcano, Montserrat, W.I. In: Druitt T, Kokelaar BP (eds), The eruption of Soufrière Hills Volcano, Montserrat, from 1995 to 1999. Mem Geol Soc London 21:363–407

Walker GPL (1983) Ignimbrite types and ignimbrite problems. J Volcanol Geotherm Res 17:65–88

Zamácola y Jaúregui JD (1804) Apuntes para la historia de Arequipa. Imp. De La Bolsa-Guañamarca, N. 49. 1888

Zora Carvajal F (1954) Tacna, Historia y Folklore. Second edition (1969), Editorial Santa María